ISSN 1062-8738, Bulletin of the Russian Academy of Sciences: Physics, 2021, Vol. 85, No. 6, pp. 658–664. © Allerton Press, Inc., 2021.
Russian Text © The Author(s), 2021, published in Izvestiya Rossiiskoi Akademii Nauk, Seriya Fizicheskaya, 2021, Vol. 85, No. 6, pp. 854–862.

Determination and Compensation of Axes Misalignment of Three-Coordinate Positioning Systems Using Acoustic Holography

D. A. Nikolaev[a], *, S. A. Tsysar[a], and O. A. Sapozhnikov[a]

[a] *Department of Physics, Moscow State University, Moscow, 119991 Russia*

**e-mail: da.nikolaev@physics.msu.ru*

Received December 9, 2020; revised January 25, 2021; accepted February 26, 2021

Abstract—Automatic positioning systems are widely used to measure acoustic fields. In practice, the orthogonality of the mechanical axes of systems can be violated during mechanical assembly and operation, producing notable errors in determining the field structure. A new way of using acoustic holography to measure angles between mechanical axes and correcting errors introduced by them is studied.

DOI: 10.3103/S1062873821060150

INTRODUCTION

Problems of using acoustic (and especially ultrasonic) fields are based on preliminary data of the spatiotemporal structure of the field, which must be known with the highest possible accuracy [1]. To find the spatial structure of an ultrasonic field, we can measure the wave parameters using a receiver (hydrophone or microphone) that moves from point to point in the considered three-dimensional area of space. An alternative faster way of recording the structure of the field is based on acoustic holography, according to which recording an acoustic signal in a two-dimensional area (within the area of a surface intersected by an ultrasonic beam) is sufficient to obtain information about the structure of the field in space [2].

These measurements require us to record a signal at a large number of points in space. In practice, the acoustic receiver is placed at specified spatial points using a positioning system with computer control. The receiving device is typically moved with high precision in such systems along some linear guides using stepper motors. There are three such guides in 3D positioning systems, positioned perpendicular to each other to form a Cartesian system of mechanical axes.

When assembling the positioner, it is not always possible to guarantee the perpendicularity of the mechanical axes with the required accuracy. The axes can be additionally skewed during the operation of the system. Since the results obtained using such systems are interpreted by assuming the mechanical axes are mutually perpendicular, the actual unknown deviation of the axes from orthogonality can introduce systematic errors in the positioning of the receiver and thus inaccurate spatial measurements of the acoustic field characteristics [3]. For example, using data obtained from measurements in a nonorthogonal coordinate system to describe the spatial structure of a field can damage healthy tissues of a patient in the therapeutic use of ultrasound [4] and result in inaccurate determination of the coordinates of acoustic scatterers in diagnostic problems [5].

If the skew angles of the mechanical axes of the positioner are known, it is easy to correct the measuring results and thereby avoid errors. The angles between the mechanical axes can be found via direct measurements using certain measuring devices. However, such measurements require the use of additional equipment, which is often inconvenient. It is also quite difficult to guarantee accuracy, especially in small positioning systems with narrow ranges of shifts along the measuring axes. In this work, we propose a new way of determining the angles between mechanical axes that is based on acoustic holography. It is similar to the approach used in [6] to characterize the acoustic properties of materials.

FORMULATION OF THE PROBLEM

The skewing of the mechanical axes of a positioning system relative to the orthogonal coordinate system is described by three angles $\alpha_1, \alpha_2, \alpha_3$ (Fig. 1a). We mark the coordinates along the skewed axes (i.e., the axes of the positioning system) with tildes. When specifying the angles, we assume that axes $0x$ and $0\tilde{x}$ coincide, axis $0\tilde{y}$ lies in plane (x, y) and forms angle α_3 with axis $0y$; the direction of axis $0\tilde{z}$ is determined by angles α_1 and α_2 of its inclination relative to planes (y, z) and (x, z), respectively.

A model experiment was performed to demonstrate the main features of the distortion of measuring results due to the skewing of the positioner axes. It was

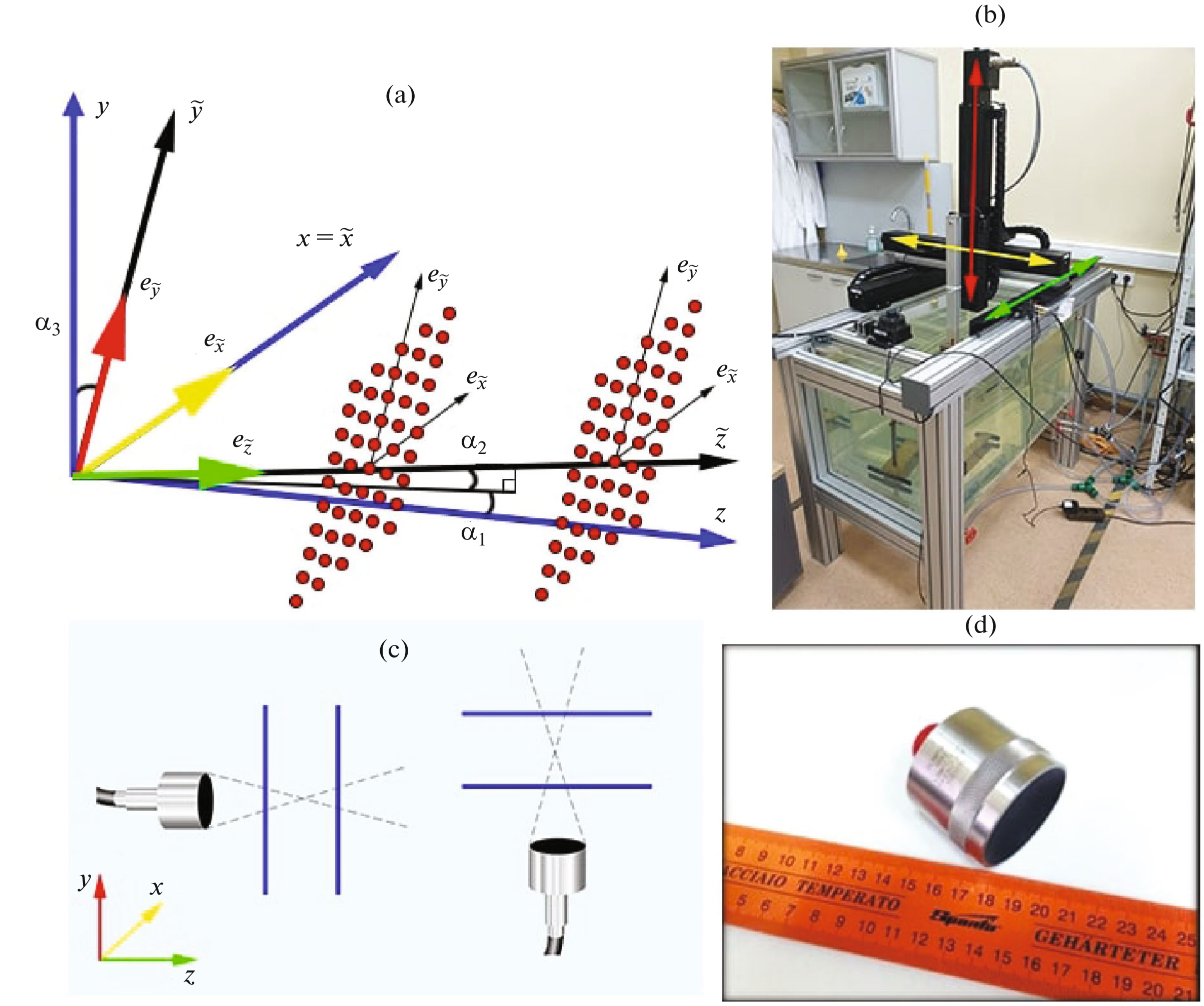

Fig. 1. (a) Orthogonal (blue axes) and nonorthogonal (black axes) coordinate systems. The coordinates in which a signal was recorded for two holograms in a nonorthogonal coordinate system are shown by red points. Angles $\alpha_1, \alpha_2, \alpha_3$ describe the nonorthogonal coordinate system relative to the orthogonal coordinate system: $\alpha_1 = \angle(y\tilde{z}, yz)$, $\alpha_2 = \angle(x\tilde{z}, xz)$, and $\alpha_3 = \angle(\tilde{y}, y)$. Positioning system: (b) two holograms were measured parallel to plane (x, y), with (c) the other two measured parallel to plane (x, z). (d) Acoustic piezoelectric transducer used in the experiment.

assumed that a two-dimensional multielement acoustic transducer in the form of a square grid with number of elements 40 × 40 lies in plane (x, y). The elements are square, $L_x = L_y = 1$ mm in size and are separated by gaps with width $d = 0.25$ mm. The amplitude of the normal component of the particle velocity within each element is assumed to be constant (a piston source). Each element irradiates in a monochromatic mode at frequency $f_0 = 2$ MHz with a different relative phase to allow electronic focusing of the acoustic field.

Two-dimensional distributions of the complex amplitude of the acoustic pressure (hologram) on a flat section parallel to the surface of the emitter at distance $z = H = 10$ mm from the emitter were calculated using the Rayleigh integral [7]. The calculations were made with and without slight skewing between the axes (i.e., at points specified by the coordinates $(x, y, z = H)$ and $(\tilde{x}, \tilde{y}, \tilde{z} = H)$. The distribution of complex amplitude of the acoustic pressure in the space in front of the two-dimensional array was then calculated using the holograms. The field was calculated from a hologram recorded at points with the coordinates of a skewed coordinate system by assuming that the corresponding signals were recorded in an ideal coordinate system. We modeled a situation where the operator of the measuring system uses a positioner with skewed axes but does not know it (or knows but ignores it). The operator therefore assumes that the positioner axes are perpendicular when he calculates the field from the hologram.

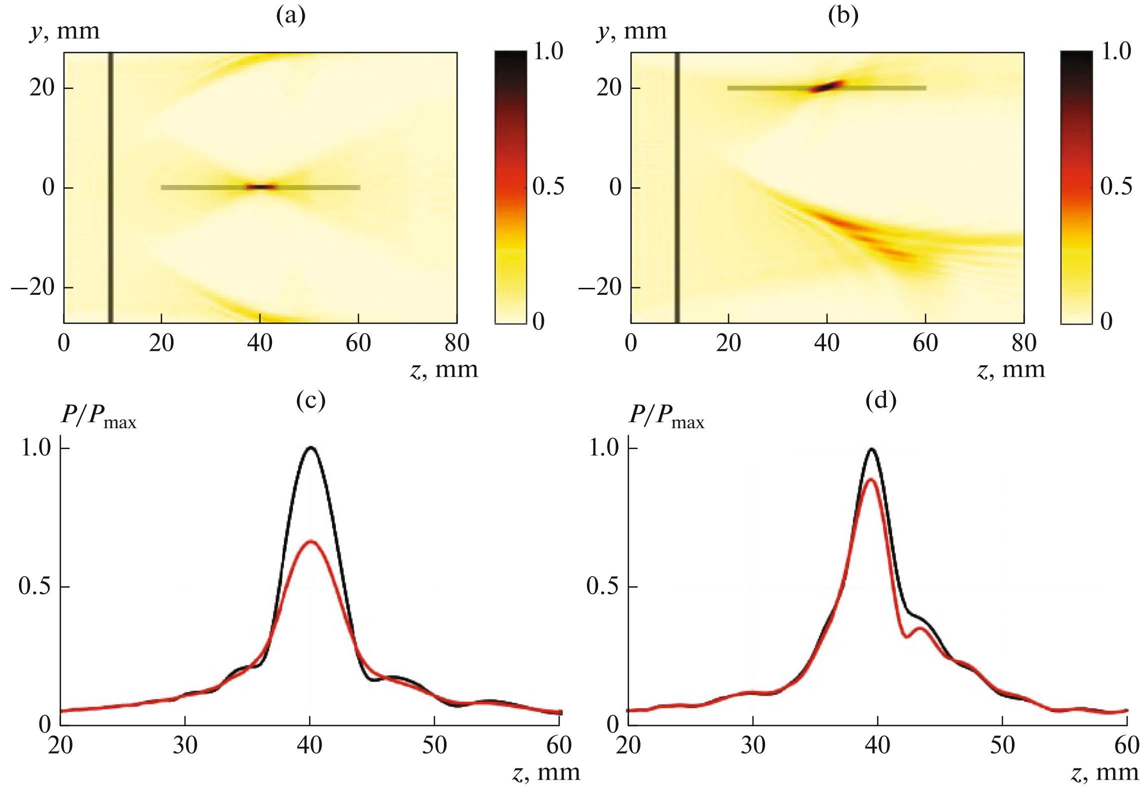

Fig. 2. Acoustic pressure of a model multielement transducer focused to points (a) (0, 0, 40 mm) and (b) (0, 20, 40 mm) . The transducer was located in plane (x, y) at $z = 0$. The position of the hologram used in the calculations is shown by the vertical line. The axis along which the pressure was distributed (Figs. 2c, 2d) is shown by the horizontal line. The pressure profiles with account for the skewing of the coordinate system axes are shown in black. The pressure profiles with no account for the skewing of the coordinate system axes are shown in red.

We considered the mode of electronic focus steering, in which the phases of signals on the radiating elements of the transducer are selected so that the emitted field is focused at a given point in space. The calculations were made for two cases of electron focusing: focusing to a point with coordinates (0, 0, 40 mm) and to a point with coordinates (0, 20, 40 mm). The corresponding normalized distributions of the amplitude of the acoustic pressure field in plane (y, z) are shown in Figs. 2a and 2b. In the first case, the skewing of the axes was set as $\alpha_1 = 1°$, $\alpha_2 = 1°$, and $\alpha_3 = 0°$. In the second, $\alpha_1 = 0°$, $\alpha_2 = 0°$, and $\alpha_3 = 1°$. Figures 2c, 2d show the amplitudes of acoustic pressure calculated along the lines (shown in Figs. 2a, 2b) from the skewed (red lines) and nonskewed (black lines) holograms. Nonzero angles α_1 and α_2 shift the entire pressure structure across axis z, and nonzero angle α_3 notably distorts the spatial structure at a distance from axis z. The skewing of the positioning system axes can thus greatly distort the measuring results and must be taken to the account.

To make the theoretical description convenient, we introduce the unit vectors of the skewed coordinate system (unit vectors codirectional with the mechanical axes of the positioning system), which we denote as $\vec{e}_{\tilde{x}}, \vec{e}_{\tilde{y}}, \vec{e}_{\tilde{z}}$. All coordinates are fixed in an undistorted coordinate system. We obtain the relation between the coordinates of the orthogonal (x, y, z) and nonorthogonal $(\tilde{x}, \tilde{y}, \tilde{z})$ coordinate systems,

$$\begin{gathered}\vec{e}_{\tilde{x}} = (1,0,0), \quad \vec{e}_{\tilde{y}} = (\sin\alpha_3, \cos\alpha_3, 0),\\ \vec{e}_{\tilde{z}} = \left(\sin\alpha_1,\ \sin\alpha_2,\ \sqrt{1-\sin^2\alpha_1-\sin^2\alpha_2}\right),\end{gathered} \tag{1}$$

$$\begin{gathered}x = \tilde{x} + \tilde{y}\sin\alpha_3 + \tilde{z}\sin\alpha_1; \quad y = \tilde{y}\cos\alpha_3 + \tilde{z}\sin\alpha_2;\\ z = \tilde{z}\sqrt{1-\sin^2\alpha_1-\sin^2\alpha_2}.\end{gathered} \tag{2}$$

Let us consider an angular spectrum for solving the Helmholtz equation for spectral amplitude $P(\omega, \vec{r})$ of acoustic pressure at an arbitrary point in the Cartesian coordinate system [8]:

$$\begin{gathered}P(\omega, x, y, z) = \left(\frac{1}{2\pi}\right)^2 \iint S_0(\omega, k_x, k_y)\\ \times e^{ik_x x + ik_y y + i\sqrt{k^2-k_x^2-k_y^2}\,z} dk_x dk_y,\end{gathered} \tag{3}$$

$$\begin{gathered}\text{where } S_0(\omega, k_x, k_y)\\ = \iint P(\omega, x, y, z=0)\, e^{-ik_x x - ik_y y} dxdy.\end{gathered} \tag{4}$$

The representation of wave field (3) is a superposition of plane waves $e^{i\vec{k}\vec{r}}$. The wave vector in the coordinate system (x, y, z) is $\vec{k} = (k_x, k_y, k_z = \sqrt{k^2 - k_x^2 - k_y^2})$, where the wave number is $k = \omega/c_0$. $S_0(\omega, k_x, k_y)$ is the angular spectrum of the field [9] in plane $z = 0$ at frequency ω. We calculate it in a skewed coordinate system using the relation between the coordinates of two systems (2). The Jacobian of the transition in Eq. (4) from variables x, y to variables $\tilde{x}, \tilde{y}$ is $\left|\frac{D(x, y)}{D(\tilde{x}, \tilde{y})}\right| = \cos\alpha_3$, so

$$S_0(\omega, k_x, k_y) = \cos\alpha_3 \iint P(\omega, \tilde{x}, \tilde{y}, \tilde{z} = 0) \times e^{-ik_x\tilde{x} - i(k_y\cos\alpha_3 + k_x\sin\alpha_3)\tilde{y}} d\tilde{x}d\tilde{y} = \cos\alpha_3 \tilde{S}_0(\omega, \tilde{k}_x, \tilde{k}_y), \quad (5)$$

$$\tilde{k}_x = k_x; \quad \tilde{k}_y = k_y\cos\alpha_3 + k_x\sin\alpha_3. \quad (6)$$

Using (2), (3), (5), and (6), we obtain the solution to the Helmholtz equation in a skewed coordinate system. The Jacobian of the transition from variables k_x, k_y to variables $\tilde{k}_x, \tilde{k}_y$ is $\left|\frac{D(k_x, k_y)}{D(\tilde{k}_x, \tilde{k}_y)}\right| = \frac{1}{\cos\alpha_3}$. We therefore obtain

$$\begin{aligned} P(\omega, \tilde{x}, \tilde{y}, \tilde{z}) &= \left(\frac{1}{2\pi}\right)^2 \iint \tilde{S}_0(\omega, \tilde{k}_x, \tilde{k}_y) e^{i\tilde{k}_x\tilde{x} + i\tilde{k}_y\tilde{y}} \\ &\times \exp\left(i\tilde{z}\left(\tilde{k}_x(\sin\alpha_1 - \tan\alpha_3\sin\alpha_2) + \frac{\sin\alpha_2}{\cos\alpha_3}\tilde{k}_y \right.\right. \\ &\left.\left. + \sqrt{k^2 - \tilde{k}_x^2 - \left(\frac{\tilde{k}_y}{\cos\alpha_3} - \tilde{k}_x\tan\alpha_3\right)^2}\right)\right) d\tilde{k}_x d\tilde{k}_y \\ &= \left(\frac{1}{2\pi}\right)^2 \iint \tilde{S}_{Z_0}(\omega, \tilde{k}_x, \tilde{k}_y) e^{i\tilde{k}_x\tilde{x} + i\tilde{k}_y\tilde{y}} d\tilde{k}_x d\tilde{k}_y. \end{aligned} \quad (7)$$

The ratio of the angular spectra measured in a skewed coordinate system on plane $\tilde{z} = Z_0$ and parallel plane $\tilde{z} = 0$ is thus

$$\begin{aligned} \Pi(\omega, \tilde{k}_x, \tilde{k}_y) &= \frac{\tilde{S}_{Z_0}(\omega, \tilde{k}_x, \tilde{k}_y)}{\tilde{S}_0(\omega, \tilde{k}_x, \tilde{k}_y)} \\ &= \exp\left[-i(\tilde{k}_x x_0 + \tilde{k}_y y_0) + iZ_0\sqrt{1 - \sin^2\alpha_1 - \sin^2\alpha_3} \right. \\ &\left. \times \sqrt{k^2 - \tilde{k}_x^2 - \left(\frac{\tilde{k}_y}{\cos\alpha_3} - \tilde{k}_x\tan\alpha_3\right)^2}\right] \\ &= \exp(i\Phi(\omega, \tilde{k}_x, \tilde{k}_y)), \end{aligned} \quad (8)$$

where $x_0 = -(\sin\alpha_1 - \tan\alpha_3\sin\alpha_2)Z_0;$

$$y_0 = -\frac{\sin\alpha_2}{\cos\alpha_3}Z_0. \quad (9)$$

Function $\Pi(\omega, \tilde{k}_x, \tilde{k}_y)$ can be considered a propagator. Values x_0, y_0 correspond to the transverse shift of a point on axis $\tilde{z}$ at distance Z_0 relative to the orthogonal coordinate system. Note that function $\Phi(\omega, \tilde{k}_x, \tilde{k}_y)$ at fixed frequency ω is a family of ellipsoidal closed curves. It does not depend on the geometry of the transducer and its location relative to the planes of the holograms. When determining the skewing of the positioning system axes, we can therefore choose a convenient transducer in terms of optimal field size, scanning time, etc. It should nevertheless be noted that phase function Φ can be determined in ranges $(\tilde{k}_x, \tilde{k}_y)$, where the amplitudes of measured angular spectra $|\tilde{S}_0(\omega, \tilde{k}_x, \tilde{k}_y)|$ and $|\tilde{S}_{Z_0}(\omega, \tilde{k}_x, \tilde{k}_y)|$ are notably different from zero. This must be considered when choosing the source of the ultrasonic field.

By measuring two holograms at different distances from the transducer, we can thus obtain a function that depends on two arguments k_x, k_y and three parameters $\alpha_1, \alpha_2, \alpha_3$. We can then calculate the angles that determine the nonorthogonal coordinate system by comparing the experimental and theoretical propagators. It is therefore possible to determine the nonorthogonality of the positioning system used for measurements.

EXPERIMENTAL

We measured the skew of the mechanical axes of the UMS-3 positioning system (Precision Acoustics, Great Britain) (Fig. 1b). Skew was introduced artificially in order to study effect of different skew angles. Three series of measurements were made in which axis $\tilde{y}$ deviated from axis y by different angles α_3. An acoustic piezoelectric transducer (Fig. 1d) with diameter $D = 38.1$ mm, focal length $F = 63.5$ mm, and an operating frequency of 1 MHz (V392, Panametrics, United States) was used in our measurements. The transducer was immersed in a tank with degassed water and positioned parallel to the hologram plane with accuracy on the order of 1°, which was achieved by preliminary alignment with respect to the mechanical axes of the positioning system on a rotary mounting platform. As noted above, function $\Phi(\omega, \tilde{k}_x, \tilde{k}_y)$ in Eq. (8) does not depend on the position of the emitter relative to the hologram, and the accuracy of the emitter's positioning does not play an important role in the approach. At the same time, it is important that the initial position does not change during measurements. This is achieved by rigidly fixing the emitter. The emitter was aligned so that the maximum possible energy of the acoustic beam for a given geometry went through the hologram's area, which is usually almost perpendicular to the acoustic axis of the emitter [10]. This allows us to obtain the highest signal-to-noise ratio at the points of the hologram.

Four holograms were recorded in one series of measurements with a given angle α_3: two holograms

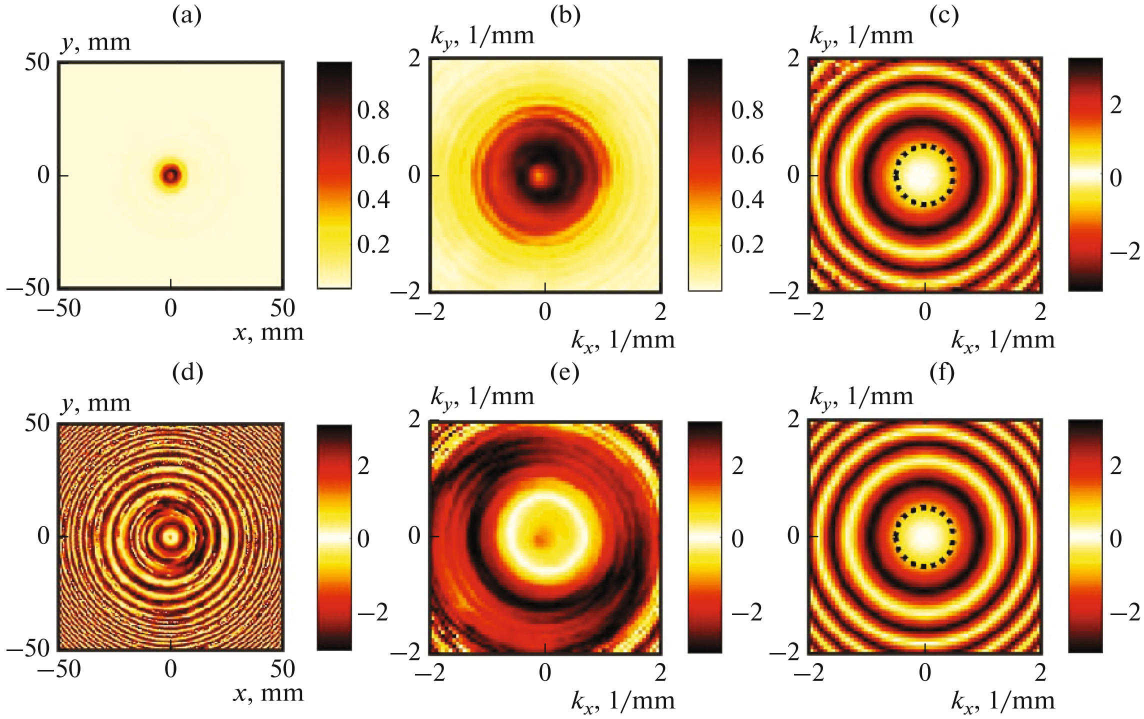

Fig. 3. Normalized (a) amplitude and (d) phase of the acoustic pressure hologram nearest to the transducer at frequency of $f =$ 1 MHz. (b) Modulus and (e) phase of the angular spectrum of the same monochromatic hologram. (c) Phase of the ratio of the far and near monochromatic hologram to the transducer of the angular spectra obtained from the experiment. (f) Phase of the theoretical ratio of angular spectra (8) at zero angles $\alpha_1, \alpha_2, \alpha_3$. The area of radius k_0 in which the angles were calculated using formula (10) is indicated by the dotted line.

were parallel to plane (x, y) with a horizontal position of the emitter axis (Fig. 1c), and two holograms were parallel to plane $(x, \tilde{z})$ with a vertical position of the transducer axis. One hologram was measured at a distance from the focus of 1.5 cm; the other hologram was measured behind the focus at the same distance. A voltage signal in the form of a radio pulse with a rectangular envelope and an amplitude of $U = 5$ V consisting of three periods of a sinusoidal signal with frequency $f_0 = 1$ MHz was applied to the emitter using a 33250A generator (Agilent, United States). The rate of repetition was $T = 4$ ms. All holograms were measured identically and had the same characteristics: size 201×201 and step $dx = dy = 0.5$ mm. The temporal waveform at each point was recorded using an HNA-0400 hydrophone (Onda, United Stated) and a TDS5034B oscilloscope (Tektronix, United States). The number of averaging at each point was $N_{\text{av}} = 48$, and the period of averaging was $T_{\text{av}} = 400$ ms. The duration of the time window was $T = 100$ μs, which ensured recording of the informative part of the signal. A discretization interval of $dt = 20$ ns provided the required frequency window size.

The spatial distributions of amplitudes and phases were obtained for all spectral components by calculating the frequency spectrum of the signal at all spatial points of the holograms (i.e., we obtained a set of monochromatic holograms). A broadband transducer was used, allowing us to use a large set of monochromatic holograms to improve the accuracy of measuring the skew angles of the axes. The hologram nearest to the transducer, in the form of the normalized amplitude and phase of the acoustic pressure at frequency $f = 1$ MHz is shown in Figs. 3a and 3d, respectively. Based on the values of the spectral density of the signal at the reference points of the hologram (e.g., in the center), we can identify the range of frequencies in which function (8) $\Phi(\omega, \tilde{k}_x, \tilde{k}_y)$ can be determined. This range was primarily due to the bandwidth of the signal emitted by the transducer. In this work, it was set in the range of $f \in (0.4, 1.6)$ MHz. There were consequently $N_f = 121$ spectral components with frequency step $df = 10$ kHz.

The corresponding angular spectra of the signal were calculated from the far and near monochromatic holograms using formula (4). The angular spectrum modulus for the hologram nearest the emitter is shown in Fig. 3b; the phase is shown in Fig. 3e. We next cal-

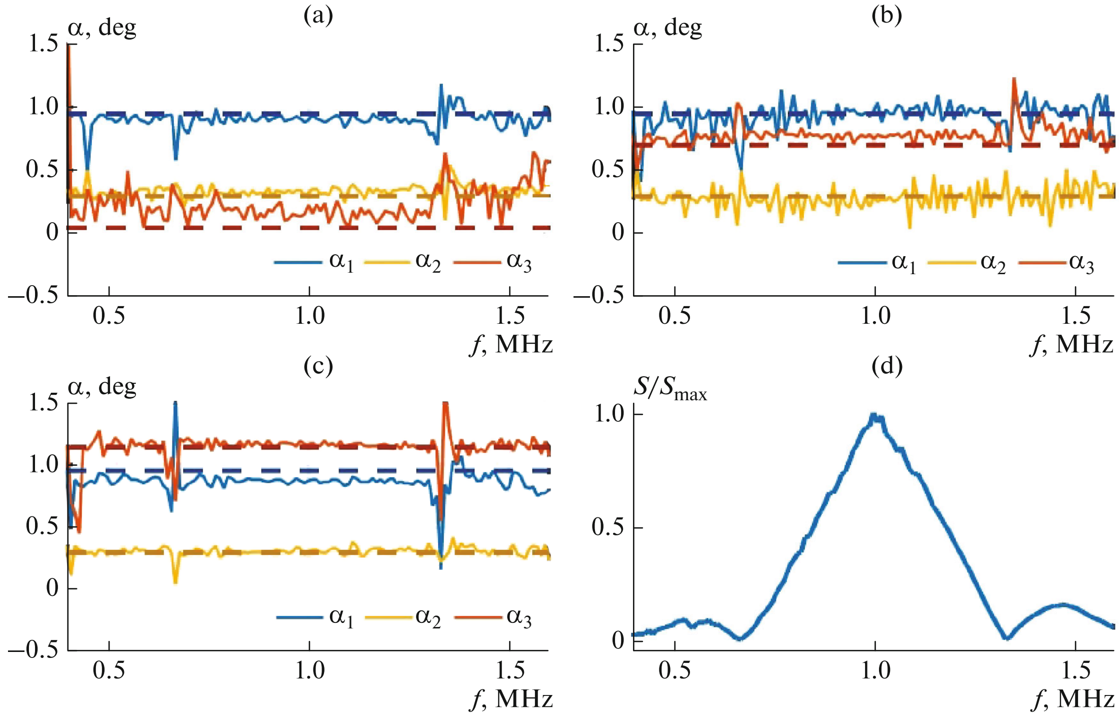

Fig. 4. Angles $\alpha_1, \alpha_2, \alpha_3$, measured using holograms at different frequencies in three series of measurements (a) with no additional skewing, (b) with additional skewing of the axis $\Delta\alpha_3 \approx 0.8°$, and (c) with additional skewing of the axis $\Delta\alpha_3 \approx 1.1°$. Angles measured geometrically with a laser system are shown by dotted lines. (d) Spectrum of the acoustic signal in the center of the near hologram.

culated the point-to-point ratio of the angular spectra, the phase of which at a frequency of 1 MHz is shown in Fig. 3c. The phase of the theoretical ratio of angular spectra (8) at zero angles $\alpha_1, \alpha_2, \alpha_3$ is shown additionally in Fig. 3f. It should be noted once again that the near and far holograms had to be measured at the same position of the emitter; changing its position between measurements of the far and near holograms would introduce an additional error in the measured angles.

Angles $\alpha_1, \alpha_2, \alpha_3$ were measured by minimizing the difference between the experimental and theoretical phases of the propagator. The angles in formula (8) for $\Phi(k_x, k_y)$ varied around zero, and the angles at which the quadratic sum of the elementwise difference between the experimental and theoretical propagator phases in a given circular area was minimal were measured:

$$\min_{\alpha_1,\alpha_2,\alpha_3} \sum_{k_x^2+k_y^2<k_0^2} \left(\Phi_{\mathrm{E}}(\omega, k_x, k_y) - \Phi_{\mathrm{T}}(\omega, k_x, k_y)\right)^2. \quad (10)$$

The radius of circle k_0 in which calculations using formula (10) were made was determined so that the frequency dispersion of the angles (Figs. 4a–4c) was minimal. At lower values of k_0, the greater dispersion was due to the small number of spatial frequencies that were used to determine angles; at higher values of k_0, the greater dispersion was due to allowing for angular components with low spectral density, which are a source of considerable random deviations. In Fig. 4, the value of k_0 was chosen so that the number of angular components falling into a circle with a radius of k_0 was $N = 225$.

This operation was performed for monochromatic holograms at different frequencies. The dependence on parameter α_3 in formula (8) is weak in contrast to α_1, α_2, and it is difficult to accurately determine α_3 from experimental holograms recorded along (x, y) at different distances z. To accurately measure all three angles that characterize the nonorthogonal (real) coordinate system, the measurements at different orientations of the hologram and the emitter relative to the positioning system (Fig. 1c) must be combined. Having two most accurately measured angles α_1 and α_2, which define the axis transverse to the hologram when it is oriented parallel to plane $(x, \tilde{y})$, and angles α_1' and α_2' when the hologram is oriented parallel to plane $(x, \tilde{z})$, angle α_3 can be measured using the following formula in the small angle approximation:

$$\alpha_3 = \arcsin\sqrt{\sin^2\alpha_1' + \sin^2\alpha_2' - \sin^2\alpha_2}. \quad (11)$$

Table 1. Skew angles of positioning system axes, obtained in three series of geometric measurements

	α_1, deg	α_2, deg	α_3, deg
No additional skewing	0.91 ± 0.03	0.33 ± 0.03	0.17 ± 0.06
Skew of $\Delta\alpha_3 \approx 0.8°$	0.96 ± 0.08	0.26 ± 0.09	0.78 ± 0.03
Skew of $\Delta\alpha_3 \approx 1.1°$	0.87 ± 0.02	0.31 ± 0.02	1.16 ± 0.02
Geometric measurements with a laser	0.95 ± 0.2 0.95 ± 0.2 0.95 ± 0.2	0.3 ± 0.2 0.3 ± 0.2 0.3 ± 0.2	0.04 ± 0.2 0.7 ± 0.2 1.14 ± 0.2

The resulting frequency dependence of three angles for three series of measurements is shown in Fig. 4. Note that the deviation of the angles from their mean values is much higher in the vicinity of frequencies $f = 0.67$–1.32 MHz than in the rest of the area. This is due to the spectral power of the signal (Fig. 4d) at these frequencies being low because of the chosen form of the supplied pulse and the characteristics of the transducer. The values of the angles at different frequencies were determined independently, so random deviations can be minimized and angle values can be obtained with high accuracy by averaging the angles in the optimum range of frequencies. The values of three angles with the standard deviation for three series of measurements are given in Table 1.

The operating range along the axes of the positioning system used in this work was quite long ($\Delta L^x_{\max} = 0.3$ m, $\Delta L^y_{\max} = 0.3$ m, $\Delta L^z_{\max} = 0.4$ m), so we measured the skew angles optically. A laser source was fixed on the positioning system, and the projections of the laser beam onto the transparent walls of the water tank were marked at extreme positions along each axis. The angle between the lines connecting opposite points lying on the same axis was determined. The results from such measurements are shown by the dashed lines in Fig. 4. They are in good agreement with the results of calculations from the holograms in Table 1. The error for the angles measured optically was determined from the size of the projected laser spot and the distance between the extreme points: $\Delta\alpha = 0.2°$. The measuring error will be greater for positioning systems with a smaller range of linear shifts.

CONCLUSIONS

The effect the nonorthogonality of a positioning system's axes has on the spatial characterization of an acoustic field was studied. A new method of determining the deviation of the positioning system axes from orthogonality was described and studied experimentally. The experimental and modeling results show that measurements at different orientations of the hologram and the transducer relative to the positioning system are needed to reliably determine the three angles of the nonorthogonal coordinate system. The angles determined in this way have a smaller error when compared to geometric measurements made by optical system. Transducer holograms measured with this positioning system can be easily corrected using the resulting data. It should also be noted that the technique can be improved by reducing the number of measurements. It is therefore necessary to measure holograms in planes that are not parallel to those formed by the axes of the positioning system.

FUNDING

This work was supported by the Russian Foundation for Basic Research, project nos. 19-32-90022 and 18-02-00991.

REFERENCES

1. Subbotin, V.G., Sapozhnikov, O.A., and Tsysar', S.A., *Sb. Tr. XXV Sessii Ross. Akust. O-va* (Proc. XXV Meetings of Russian Acoust. Soc.), 2012, vol. 2, p. 123.
2. Sapozhnikov, O.A., Tsysar, S.A., Khokhlova, V.A., et al., *J. Acoust. Soc. Am.*, 2015, vol. 138, no. 3, p. 1515.
3. Kreider, W., Khokhlova, V., Tsysar, S., et al., *J. Acoust. Soc. Am.*, 2017, vol. 141, no. 5, p. 4009.
4. Pye, S.D., *Physiotherapy*, 1996, vol. 82, no. 1, p. 39.
5. Sukhoruchkin, D.A., Yuldashev, P.V., Tsysar, S.A., et al., *Bull. Russ. Acad. Sci.: Phys.*, 2018, vol. 82, no. 5, p. 507.
6. Nikolaev, D., Tsysar, S., Krendeleva, A., et al., *Proc. Meet. Acoust.*, 2019, vol. 38, no. 1, 045012.
7. Cathignol, D. and Sapozhnikov, O.A., *Acoust. Phys.*, 1999, vol. 45, no. 6, p. 735.
8. Vinogradova, M.B., Rudenko, O.V., and Sukhorukov, A.P., *Teoriya voln* (Wave Theory), Moscow: Nauka, 1979.
9. Schafer, M.E. and Lewin, P.A., *J. Acoust. Soc. Am.*, 1989, vol. 85, no. 5, p. 2202.
10. Marhenke, T., Sanabria, S.J., Chintada, B.R., et al., *Sensors*, 2019, vol. 19, p. 863.

Translated by I. Obrezanova